

## DELAYED PROTONS FOLLOWING $^{21}\text{Mg}$ AND $^{25}\text{Si}$ DECAY

R. MCPHERSON\* AND J. C. HARDY

*Foster Radiation Laboratory, McGill University, Montreal†*

Received August 10, 1964

### ABSTRACT

The delayed-proton precursors  $^{21}\text{Mg}$  and  $^{25}\text{Si}$  have been produced by proton bombardment of targets of sodium, magnesium, aluminum, and silicon dioxide in the internal beam of the McGill synchrocyclotron. Half-lives of  $118 \pm 4$  and  $225 \pm 6$  msec respectively were measured, and a spin-parity assignment of  $(5/2)^+$  has been made to the ground state of  $^{21}\text{Mg}$ . Strong lines in the delayed-proton spectra have been attributed to decay of the expected first  $T = 3/2$  states in  $^{21}\text{Na}$  and  $^{25}\text{Al}$ , fed by superallowed  $\beta$  transitions from the respective precursors  $^{21}\text{Mg}$  and  $^{25}\text{Si}$ .

### INTRODUCTION

A neutron-deficient nuclide, bound in its ground state and having a  $Q$  value for  $\beta$  decay larger than the proton separation energy of its  $\beta$ -decay daughter, can lead to delayed proton emission from unbound excited states of the daughter. The energetics of a large number of new neutron-deficient nuclides which meet these conditions have been predicted using isobaric invariance principles and known masses of neighboring or mirror nuclei (e.g. Goldansky 1960; Jaenecke 1964). Observation of the proton transitions from daughter states provides an easy method of identification for many of these short-lived nuclides.

As neutrons are removed from stable isotopes of the elements between oxygen and calcium, the first-encountered delayed-proton precursors are the  $T_z = -3/2$  nuclides  $^{13}\text{O}$ ,  $^{17}\text{Ne}$ ,  $^{21}\text{Mg}$ ,  $^{25}\text{Si}$ ,  $^{29}\text{S}$ ,  $^{33}\text{Ar}$ , and  $^{37}\text{Ca}$ . Each of these can be produced by removal of at most three neutrons in proton-induced reactions on the lightest corresponding stable isotopes. For the members of this group heavier than  $^{17}\text{Ne}$ , the possibility exists of having a large  $\beta$ -decay component corresponding to superallowed transitions to the first  $T = 3/2$  states of the  $T_z = -1/2$  daughters. Narrow proton lines due to transitions from the  $T = 1/2$  admixture in these states should then dominate the delayed proton spectra.

Delayed protons attributed to four of these nuclides ( $^{13}\text{O}$ ,  $^{17}\text{Ne}$ ,  $^{21}\text{Mg}$ , and  $^{25}\text{Si}$ ) have been observed by Barton *et al.* (1963). In each case, poorly resolved

\*Now at Chemistry Department, Brookhaven National Laboratories.

†The laboratory was formally named The John Stuart Foster Radiation Laboratory by order of the Board of Governors of McGill University in June, 1964.

proton groups were fitted to known levels in the  $\beta$ -decay daughters. A later work, also from this laboratory (McPherson, Hardy, and Bell 1964), provides a more detailed study of the  $^{17}\text{Ne}$  decay. The present paper describes the results of improved measurements on  $^{21}\text{Mg}$ , produced by proton reactions in targets of sodium and magnesium, and on  $^{25}\text{Si}$ , produced in targets of aluminum and silicon. With improved knowledge of the proton spectra, some parts of the decay schemes of  $^{21}\text{Mg}$  and  $^{25}\text{Si}$  proposed by Barton *et al.* (1963) have been modified.

#### EXPERIMENTAL TECHNIQUE

Proton bombardments of thin target foils were performed in the internal beam of the McGill synchrocyclotron. Figure 1 shows the configuration of a thin target foil and solid-state detector mounted on the end of a radial probe.

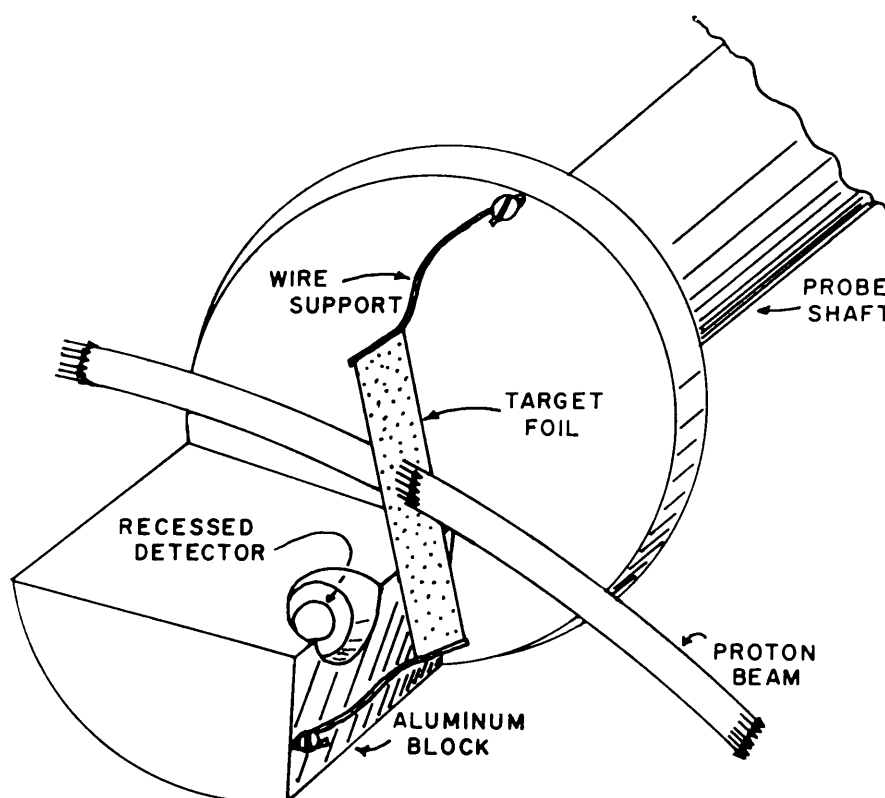


FIG. 1. Experimental configuration as mounted on the end of a radial probe and inserted into the internal cyclotron beam.

The probe could be inserted into the circulating beam at radii corresponding to proton energies between 30 and 98 MeV, and depending on the radius chosen for bombardment, the beam traversed the target from 10 to 50 times, giving an effective current of some tens of microamperes. The target foil was suspended 6 cm from the detector and intercepted the proton beam in the median plane. A silicon surface barrier detector of 200-mm<sup>2</sup> area was enclosed in an aluminum shield suspended below the median plane and was connected, through the probe, to an Ortec charge-sensitive preamplifier outside the region of strongest magnetic field. The detector depletion depth of 300 microns allowed measurement of full energy for protons up to 6 MeV. Aluminum absorber foils over the detector were used to protect it from unwanted ion

bombardment and, by varying their number, to measure the specific ionization of the detected particles.

Counting was performed between repetitive bursts—typically 40 msec long—of normal cyclotron operation. A clock-controlled counting period was initiated following a 100-msec delay which was long enough to allow dissipation of beam storage effects in the cyclotron; it was found that shorter delays resulted in a large background continuum appearing under the delayed-proton spectrum. Usually the spectrum, taken over the total counting period, was stored in one half of a 256-channel analyzer. For lifetime runs, however, the counting period was divided accurately into four equal intervals and the spectra corresponding to each were stored sequentially in the four quarters of the analyzer memory. Thus four-point decay curves for the peaks in the spectrum could be obtained. The duration of the counting period depended on the lifetime of the delayed protons and on whether or not decay curves were being sought, but it was usually less than half a second.

Pulses from a mercury pulse generator were fed onto the input of the pre-amplifier, and were used in conjunction with the  $^{210}\text{Po}$   $\alpha$  line to calibrate the energy response of the system. The resolution for the 5.3-MeV  $\alpha$ 's was 76 keV FWHM.

#### EXPERIMENTAL RESULTS

##### $^{21}\text{Mg}$ : Identification

Figure 2 shows the delayed-proton spectrum obtained following the bombardment of a 2.3-mg/cm<sup>2</sup> foil of natural magnesium; the total counting time

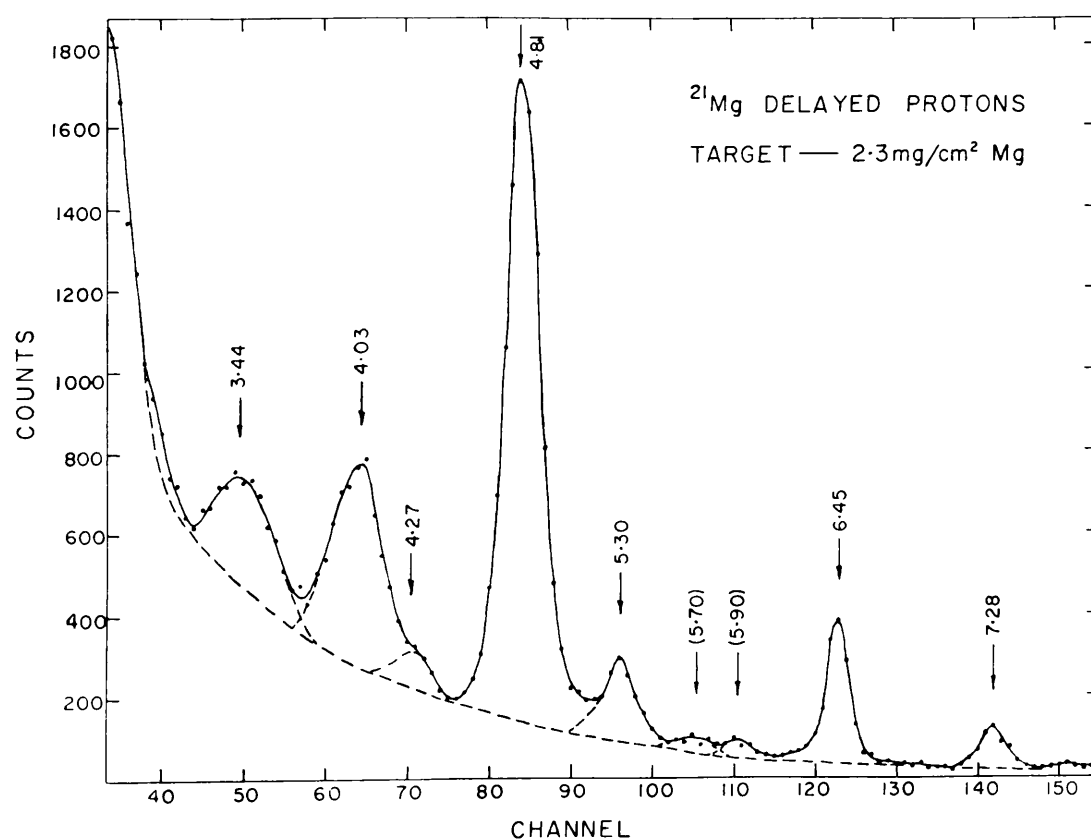


FIG. 2. Spectrum of delayed protons following the decay of  $^{21}\text{Mg}$ . The energy of each proton peak is shown in MeV, corrected to center of mass.

was 25 minutes. A somewhat thicker sodium target yielded a similar spectrum, although the peaks were necessarily less well resolved. Both targets were bombarded at incident proton energies from threshold to 85 MeV, and at each energy the delayed spectrum remained qualitatively unchanged. Since lifetime measurements also indicated that all major peaks had the same half-life, within experimental error, it may be concluded that the delayed protons all follow the  $\beta$  decay of the same nuclide.

Yield curves were plotted for both targets by measuring the production of the main peak as a function of the target radius in the cyclotron. Radial oscillations in the cyclotron beam make the actual bombarding energy at a given target radius less than the nominal cyclotron energy at that radius by an amount that is not well determined (2 to 5 MeV), but relative threshold measurements are accurate to better than 2 MeV. Since the proton peaks of Fig. 2 were not observed when a fluorine target was used (McPherson *et al.* 1964), the nuclide responsible for the present activity must be an isotope of magnesium or sodium. Any isotope of sodium that can be a delayed-proton precursor must have a production threshold from stable magnesium lower than that from sodium. In fact, the production threshold from magnesium was 8 MeV greater than that from sodium, and was approximately 50 MeV. These results are compatible only with the reactions  $^{24}\text{Mg}(p, d2n)^{21}\text{Mg}$  and  $^{23}\text{Na}(p, 3n)^{21}\text{Mg}$ , whose calculated laboratory energy thresholds, based on the estimated  $Q_{\beta^+}$  of  $(13.0 \pm 0.3)$  MeV for  $^{21}\text{Mg}$  made by Jaenecke (1964), are  $(48.6 \pm 0.3)$  and  $(38.9 \pm 0.3)$  MeV respectively. This verifies the assignment of this activity to  $^{21}\text{Mg}$  by Barton *et al.* (1963).

#### $^{21}\text{Mg}$ : Half-life

Typical four-point decay curves appear in Fig. 3 and represent the decay of individual proton lines as indicated. Similar curves have been obtained for other prominent energy peaks and, together with the three illustrated, allow us to adopt the value  $(118 \pm 4)$  msec for the half-life of  $^{21}\text{Mg}$ .

#### $^{21}\text{Mg}$ : Energies and Decay Scheme

The energies shown in Fig. 2 appear also in the first column of Table I; they are corrected to center of mass and have the indicated uncertainties.

TABLE I

Known and proposed new levels of  $^{21}\text{Na}$  as indicated by the experimental data; three of the four proposed levels appear twice since they are indicated by two proton groups

$E_p$ (c. of m.), MeV	$E_p + (^{20}\text{Ne} + p)$ , MeV	$E_p + (^{20}\text{Ne}^* + p)$ , MeV	Levels in $^{21}\text{Na}$ , MeV	
			Known†	Proposed
$3.44 \pm 0.06$	$5.89 \pm 0.06$	$7.52 \pm 0.06$	7.45	
$4.03 \pm 0.06$	$6.48 \pm 0.06$	$8.11 \pm 0.06$	6.52	
$4.27 \pm 0.08$	$6.72 \pm 0.08$	$8.35 \pm 0.08$		$8.35 \pm 0.08$
$4.81 \pm 0.04$	$7.26 \pm 0.04$	$8.89 \pm 0.04$		$8.90 \pm 0.04$
$5.30 \pm 0.04$	$7.75 \pm 0.04$	$9.38 \pm 0.04$		$7.75 \pm 0.04$
$(5.70) \pm 0.1$	$(8.15) \pm 0.1$	$(9.78) \pm 0.1$		$9.73 \pm 0.06$
$(5.90) \pm 0.1$	$(8.35) \pm 0.1$	$(9.98) \pm 0.1$		$8.35 \pm 0.08$
$6.45 \pm 0.04$	$8.90 \pm 0.04$	$10.53 \pm 0.04$		$8.90 \pm 0.04$
$7.28 \pm 0.06$	$9.73 \pm 0.06$	$11.36 \pm 0.06$		$9.73 \pm 0.06$

†See Endt and van der Leun (1962).

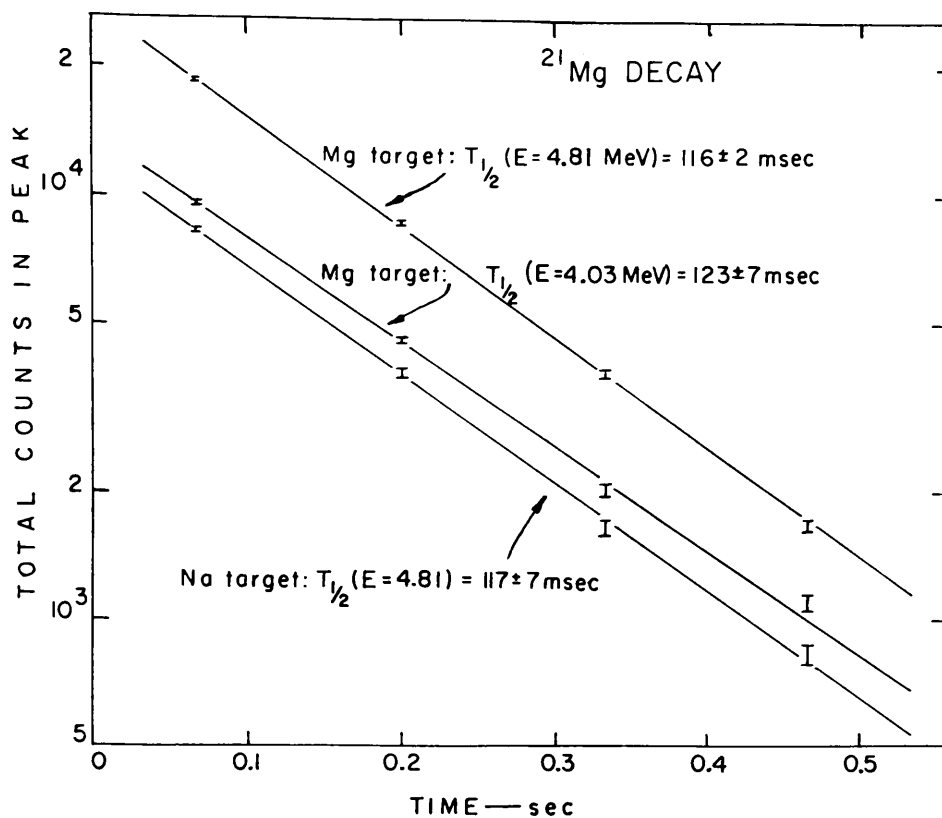


FIG. 3. Typical four-point decay curves for peaks in the spectrum of protons following  $^{21}\text{Mg}$ . The target used, the energy of the peak considered, and the measured half-life are indicated for each curve.

Column 2 in that table gives the predicted energy of the corresponding level in  $^{21}\text{Na}$  assuming that proton decay proceeds to the ground state of  $^{20}\text{Ne}$ , and column 3 gives the same quantity assuming that the decay proceeds to the first excited state of  $^{20}\text{Ne}$ . The italicized energy values are those which appear to correspond to actual level energies in  $^{21}\text{Na}$ . Two of the proton peaks can be seen to fit approximately the proton decay of known  $^{21}\text{Na}$  levels at 6.52 and 7.45 MeV. Three proposed new levels at 8.35, 8.90, and 9.73 MeV can be assigned with some certainty since their decay to the ground and first excited states of  $^{20}\text{Ne}$  would give rise to proton energies agreeing with observed peaks. The remaining peak at 5.30 MeV has been tentatively assigned to an additional proposed level at 7.75 MeV which is assumed to decay predominantly to the  $^{20}\text{Ne}$  ground state. The proposed decay scheme is shown in Fig. 4 and includes all known levels for  $^{21}\text{Na}$  that appear in the compilation of Endt and van der Leun (1962).

Kienle and Wien (1963) have assigned a spin-parity of  $(5/2+)$  to the ground state of  $^{21}\text{F}$ , the mirror nucleus of  $^{21}_{12}\text{Mg}$ . If, as seems likely, the ground state of  $^{21}\text{Mg}$  is also  $5/2+$ , then within the observable energy range (i.e., levels above about 5.3 MeV) the only  $^{21}\text{Na}$  level with known spin-parity which must be excited by an allowed  $\beta$  transition is the one at 6.52 MeV; the other known level in Table I has not been assigned any spin. Within the same range of energy, there are six remaining known levels which have apparently not been excited; of these, three have known spin-parities which, on the basis of  $5/2+$  for  $^{21}\text{Mg}$ , preclude their being excited by allowed  $\beta$  transitions, and the others have no assigned spin-parity. Thus, the proposed decay scheme is quite consistent with respect to previously observed levels and seems to demand

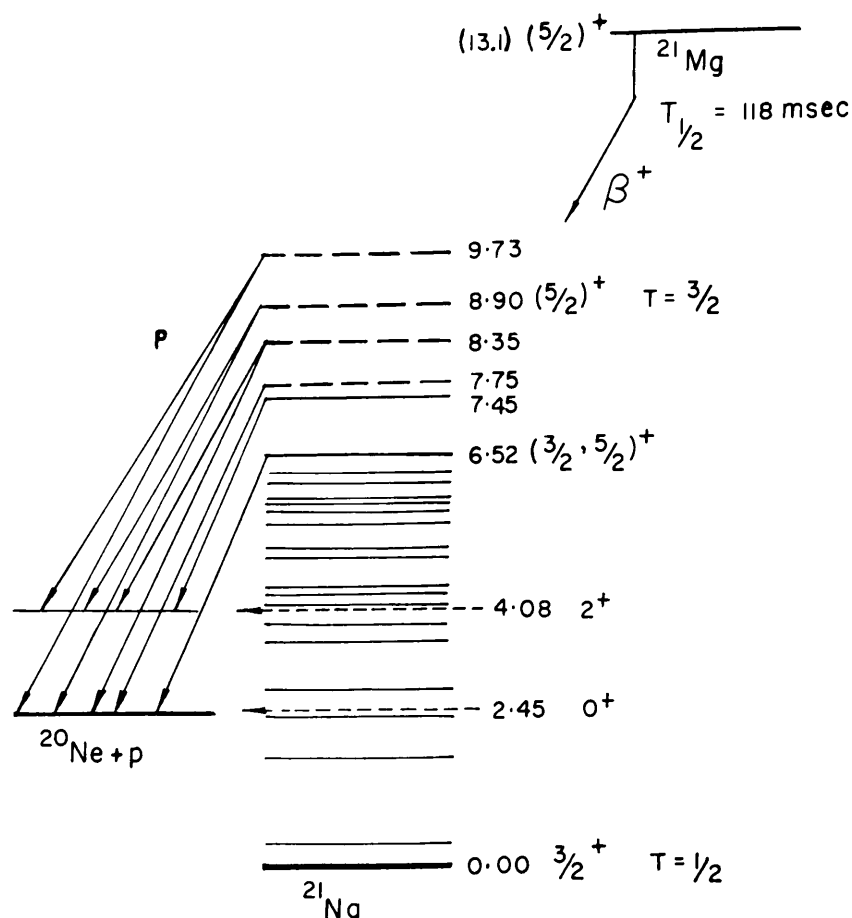


FIG. 4. Proposed decay scheme of  $^{21}\text{Mg}$ . The  $T = 3/2$  level is shown dashed at  $8.90 \text{ MeV}$ ; all other levels and assignments in  $^{21}\text{Na}$  are from the compilation of Endt and van der Leun (1962).

$5/2+$  for the spin-parity of  $^{21}\text{Mg}$ . Oda *et al.* (1959) suggest  $(5/2+)$  as the spin-parity of the  $7.45\text{-MeV}$  level in  $^{21}\text{Na}$  but consider  $(3/2+)$ ,  $(5/2-)$ , and  $(3/2-)$  also as possibilities; our results tend to confirm a  $(5/2+)$  or  $(3/2+)$  assignment to that level.

Using the semiempirical formula of Jaenecke (1960) for the Coulomb energy difference between  $^{21}\text{F}$  and  $^{21}\text{Ne}$ , it is possible to estimate an excitation energy of  $(8.7 \pm 0.5) \text{ MeV}$  for the first  $T = 3/2$  level in  $^{21}\text{Ne}$ . Accepting isobaric invariance, one then expects the lowest  $T = 3/2$  level in  $^{21}\text{Na}$  at about this energy. A  $\Delta T = 0$  superallowed  $\beta$  transition should occur from the  $T = 3/2$  ground state of  $^{21}\text{Mg}$  to this analogue level.

Relative  $\log ft$  values for  $\beta$  decay to the levels at  $8.90$  and  $9.73 \text{ MeV}$  may be estimated since the energies and thus relative intensities of all their possible proton decays are within the range of observation. Assuming that the  $\beta$  decay to the  $9.73\text{-MeV}$  level represents an ordinary allowed transition, one may suppose that its  $\log ft$  value is between  $4.0$  and  $5.0$ . On the basis of comparative total proton intensities, the  $\log ft$  for  $\beta$  decay to the  $8.90\text{-MeV}$  level then lies between  $2.8$  and  $3.8$ , indicative of a superallowed transition. The same conclusion follows from assuming any other of the observed levels to be excited by allowed  $\beta$  transitions of the same  $\log ft$  range.

We thus assign the 8.90-MeV level as the lowest  $T = 3/2$  level in  $^{21}\text{Na}$ , the analogue to the ground state of  $^{21}\text{Mg}$ . This assignment is quite consistent with its nonappearance in the resonance data for proton reactions on  $^{20}\text{Ne}$ . In this energy region, the  $T = 1/2$  isotopic spin impurity of the level may remain small and so it would be only weakly excited in such a reaction. In fact such a weak admixture, which would result in particularly narrow proton peaks, seems indicated by our results: the widths of the peaks at 4.81 and 6.45 MeV can be accounted for by the resolution of the detector and the energy spread in the target. Other peaks in the spectrum appear to be marginally wider, perhaps indicating widths of a few tens of keV for the emitting levels.

Using the value of 8.90 MeV for the lowest  $T = 3/2$  state of  $^{21}\text{Na}$  and the calculated Coulomb energy difference, a revised estimate of the  $Q_{\beta^+}$  of  $^{21}\text{Mg}$  is  $(13.1 \pm 0.2)$  MeV.

#### $^{25}\text{Si}$ : Identification

Figure 5 shows the spectrum obtained from a 2.4-mg/cm<sup>2</sup> target of aluminum; a 3.0-mg/cm<sup>2</sup> silicon dioxide target produced a similar result. At bombarding energies from threshold to 85 MeV, the spectrum remained qualitatively

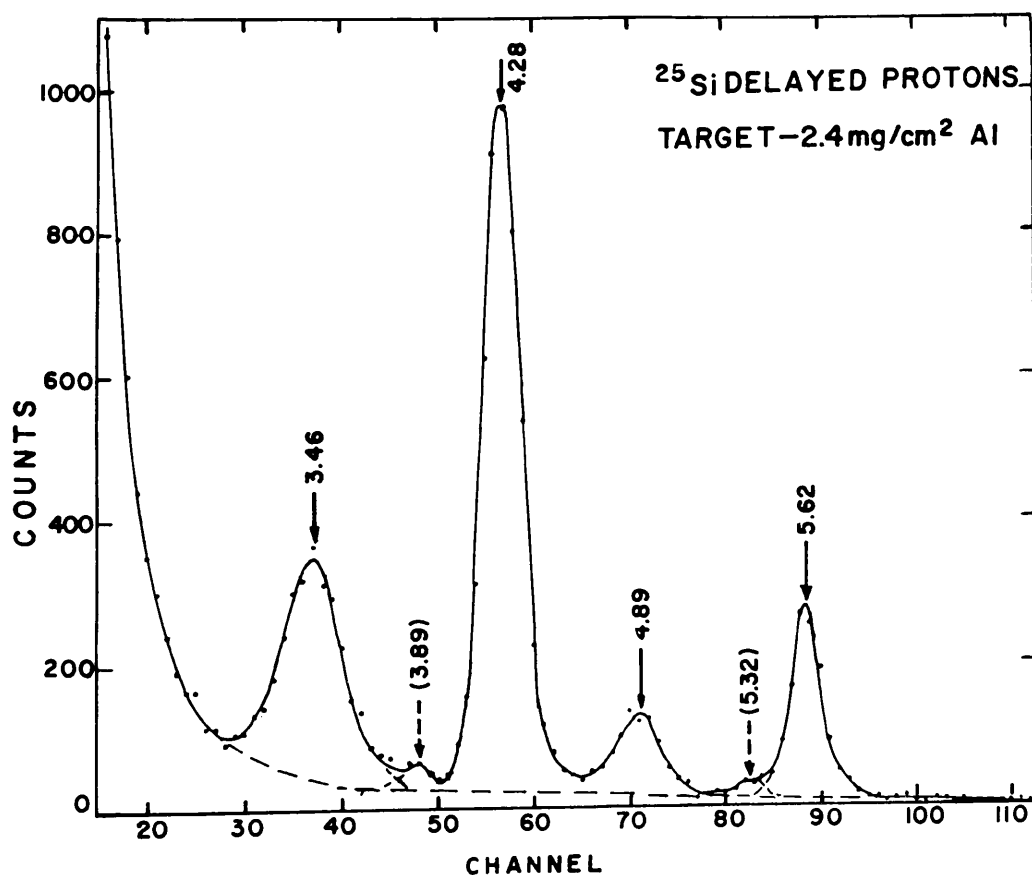


FIG. 5. Spectrum of delayed protons following the decay of  $^{25}\text{Si}$ . The energy of each proton peak is shown in MeV, corrected to center of mass.

unchanged. Lifetime measurements on the four largest-intensity peaks indicated no significant difference between them, and it was concluded that the delayed protons in these four peaks all follow the decay of the same nuclide. The two

low-intensity peaks at 3.89 and 5.32 MeV were not sufficiently above background to allow positive identification of their source. Since the spectrum from a magnesium target was completely different, the nuclide responsible for the activity in Fig. 5 is restricted to an isotope of either aluminum or silicon. Yield curves for production of the major peak from both targets showed that the production threshold from silicon was 8 MeV greater than from aluminum and was approximately 50 MeV. This case is similar to that for  $^{21}\text{Mg}$ , and the results are only compatible with the reactions  $^{28}\text{Si}(p, d2n)^{25}\text{Si}$  and  $^{27}\text{Al}(p, 3n)^{25}\text{Si}$ , whose calculated laboratory energy thresholds, based on the estimate of Jaenecke for the  $Q_{\beta+}$  of  $^{25}\text{Si}$  (12.6 MeV), are  $(48.9 \pm 0.5)$  and  $(39.2 \pm 0.5)$  MeV.

#### $^{25}\text{Si}$ : Half-life

Typical decay curves are shown in Fig. 6. From such measurements we adopt the value  $(225 \pm 6)$  msec for the half-life of  $^{25}\text{Si}$ .

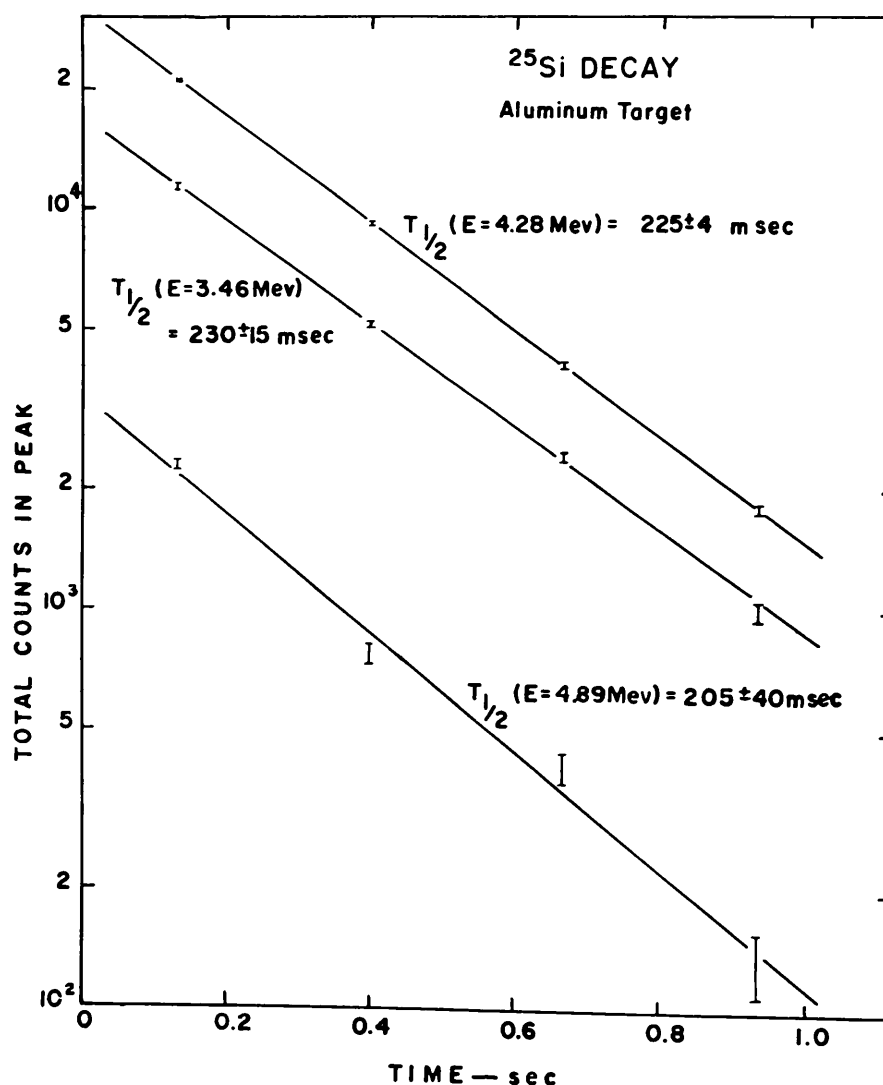


FIG. 6. Typical four-point decay curves for peaks in the spectrum of protons following  $^{25}\text{Si}$ . The energy of the peak considered and its measured half-life are indicated for each curve.

#### $^{25}\text{Si}$ : Energies and Decay Scheme

Table II shows the proton energies (corrected to center of mass) which were taken from Fig. 5. Like Table I, it shows in columns 2 and 3 the level



energies in  $^{25}\text{Al}$  which would result in the observed proton peaks, supposing decay to the ground or first excited state, respectively, of  $^{24}\text{Mg}$ . Two of the proton peaks fit the decay of the known spin  $(3/2)$  level at 7.14 MeV; the two small peaks, if they are in fact from  $^{25}\text{Al}$ , could fit an uncertain level at 7.5 MeV. The remaining two are consistent with the existence of a new level at 7.93 MeV. The proposed decay scheme is shown in Fig. 7.

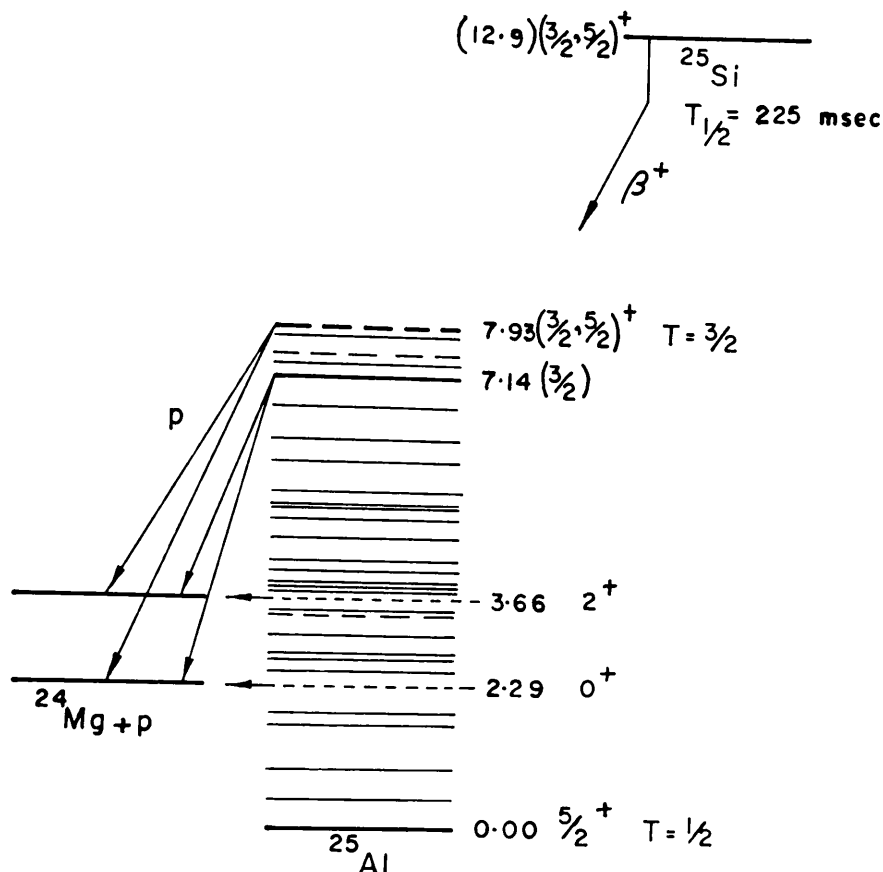


FIG. 7. Proposed decay scheme of  $^{25}\text{Si}$ . The  $T = 3/2$  level is shown dashed at 7.93 MeV; all other levels and assignments in  $^{25}\text{Al}$  are from the compilation of Endt and van der Leun (1962). If the two small peaks in Fig. 5 are to appear in this scheme, they will run from the dashed level at 7.5 MeV to the ground and first excited states of  $(^{24}\text{Mg} + p)$ .

TABLE II  
Agreement between predicted and known levels in  $^{25}\text{Al}$

$E_p$ (c. of m.), MeV	$E_p + (^{24}\text{Mg} + p)$ , MeV	$E_p + (^{24}\text{Mg}^* + p)$ , MeV	Levels in $^{25}\text{Al}$ , MeV	
			Known†	Proposed
$3.46 \pm 0.06$	$5.75 \pm 0.06$	$7.12 \pm 0.06$	7.14	
$(3.89) \pm 0.1$	$(6.18) \pm 0.1$	$(7.55) \pm 0.1$	(7.5)	
$4.28 \pm 0.04$	$6.57 \pm 0.04$	$7.94 \pm 0.04$		$7.93 \pm 0.04$
$4.89 \pm 0.06$	$7.18 \pm 0.06$	$8.55 \pm 0.06$	7.14	
$(5.32) \pm 0.08$	$(7.61) \pm 0.08$	$(8.98) \pm 0.08$	(7.5)	
$5.62 \pm 0.04$	$7.91 \pm 0.04$	$9.28 \pm 0.04$		$7.93 \pm 0.04$

†See Endt and van der Leun (1962).

The ground state of  $^{25}\text{Si}$  could be either  $3/2+$  or  $5/2+$ , although the fact that the mirror nucleus,  $^{25}\text{Na}$ , has a spin-parity of  $5/2+$  makes the latter value more likely. Within the observable energy range (i.e. levels above about

5.4 MeV) there are seven known levels in  $^{25}\text{Al}$ , of which only one has definite spin-parity and to this level allowed  $\beta$  decay is not possible. Thus, in the absence of known spin-parity information, the proposed decay scheme is quite consistent with respect to previously observed levels, but does not allow us to decide between  $3/2+$  and  $5/2+$  for  $^{25}\text{Si}$ .

The proposed level at 7.93 MeV in  $^{25}\text{Al}$  appears to be the expected first  $T = 3/2$  level. Using the semiempirical Coulomb energy difference between  $^{25}\text{Na}$  and  $^{25}\text{Mg}$ , it is possible to predict the energy of this level in  $^{25}\text{Al}$  as  $(7.6 \pm 0.5)$  MeV. Relative  $\log ft$  values for  $\beta$  decay to the levels at 7.93 and 7.14 MeV may be estimated by comparing the sum of intensities of the two proton groups from each level; i.e., the sum of intensities of peaks at 3.46 and 4.89 MeV is compared with the sum of intensities of peaks at 4.28 and 5.62 MeV. Assuming, as was done for  $^{21}\text{Mg}$ , that  $\beta$  decay to the level at 7.14 MeV is allowed, its  $\log ft$  value could lie between 4.0 and 5.0. In this case, the  $\log ft$  value for  $\beta$  decay to the 7.93-MeV level would be between 3.3 and 4.3, indicative of a superallowed  $\beta$  transition. Again, consistent with the  $T = 3/2$  assignment, the widths of the proton transitions from this level are the narrowest in the spectrum and can be accounted for by instrumental resolution and target thickness.

The calculated Coulomb energy difference between  $^{25}\text{Si}$  and  $^{25}\text{Al}$  can be applied to give a revised estimate of  $(12.9 \pm 0.2)$  MeV for the  $Q_{\beta+}$  of  $^{25}\text{Si}$ .

#### SUMMARY

The observation of delayed proton spectra following the decay of the neutron-deficient nuclides  $^{21}\text{Mg}$  and  $^{25}\text{Si}$  has led to results which are summarized in Table III. Work is being undertaken to explore the decays of the remaining  $T_z = -3/2$  nuclides between oxygen and calcium.

TABLE III  
Summary of results

Parent nuclide	$J\pi$	$Q_{\beta+}$ (est.), MeV	$T_{1/2}$ , msec	Energy of lowest $T = 3/2$ state of daughter, MeV
$^{21}\text{Mg}$	$(5/2)+$	$13.1 \pm 0.2$	$118 \pm 4$	$8.90 \pm 0.04$ ( $^{21}\text{Na}^*$ )
$^{25}\text{Si}$		$12.9 \pm 0.2$	$225 \pm 6$	$7.93 \pm 0.04$ ( $^{25}\text{Al}^*$ )

#### ACKNOWLEDGMENTS

The authors received financial assistance from the National Research Council of Canada in the form of Studentships held during the course of this work. The research was supported by a grant from the Atomic Energy Control Board.

We should also like to thank the director of the laboratory, Dr. R. E. Bell, for a number of helpful discussions.

## REFERENCES

- BARTON, R., MCPHERSON, R., BELL, R. E., FRISKEN, W. R., LINK, W. T., and MOORE, R. B.  
1963. *Can. J. Phys.* **41**, 2007.  
ENDT, P. M. and VAN DER LEUN, C. 1962. *Nucl. Phys.* **34**, 1.  
GOLDANSKY, V. I. 1960. *Nucl. Phys.* **19**, 482.  
JAENECKE, J. 1960. *Z. Physik*, **160**, 171.  
——— 1964. *Nucl. Phys.* (to be published).  
KIENLE, P. and WIEN, K. 1963. *Nucl. Phys.* **41**, 608.  
MCPHERSON, R., HARDY, J. C., and BELL, R. E. 1964. *Phys. Letters*, **10**, 65.  
ODA, Y., TAKEDA, M., HU, C., and KATO, S. 1959. *J. Phys. Soc. Japan*, **14**, 396.